



# Sea-Ice Permittivity Estimation using GNSS Reflectometry data of the MOSAiC Expedition

M. Semmling (1), J. Wickert (2), S. Gerland (3), D. Divine (3), F. Kreß (4), M. Hoque (1), G. Spreen (5)

(1) German Aerospace Centre, Institute for Solar-Terrestrial Physics (DLR-SO)

(2) German Research Centre for Geosciences (GFZ)

(3) Norwegian Polar Institute (NPI), Fram Centre

(4) Technische Universität Berlin, Institute of Geodesy and Geoinformation Science

(5) University of Bremen, Institute of Environmental Physics



## Abstract

Sea ice is a crucial parameter of the Earth climate system. Its high albedo compared to water influences the oceans' radiation budget significantly. The importance of monitoring arises from the high variability of sea-ice state and amount induced by seasonal change and global warming. GNSS reflectometry can contribute to global monitoring of sea ice with high potential to extend the spatio-temporal coverage of today's observation techniques. Properties like ice salinity, temperature and thickness can affect the signal reflection. The MOSAiC expedition (Multidisciplinary drifting Observatory for the Study of Arctic Climate) gave us the opportunity to conduct reflectometry measurements under different sea-ice conditions in the central Arctic. A dedicated setup was mounted, in close cooperation with the Alfred-Wegener-Institute (AWI), on the German research icebreaker *Polarstern* that drifted for one year with the Arctic sea ice. We present results from data recorded between autumn 2019 and spring 2020. The ship drifted from the marginal ice zone (MIZ) in the Siberian sector of the Arctic (starting in September 2019), over the compact ice zone (CIZ) in the central Arctic towards Svalbard (reached in June 2020). Profiles of sea-ice reflectivity over elevation angle (range:  $1^\circ$  to  $45^\circ$ ) are derived with daily resolution considering reflection data recorded at left-handed (LH) and right-handed (RH) circular polarization. Relative permittivity estimates of the ice-covered ocean are obtained for the 8-month period with daily resolution.

## MOSAIC Measurements and Retrieval

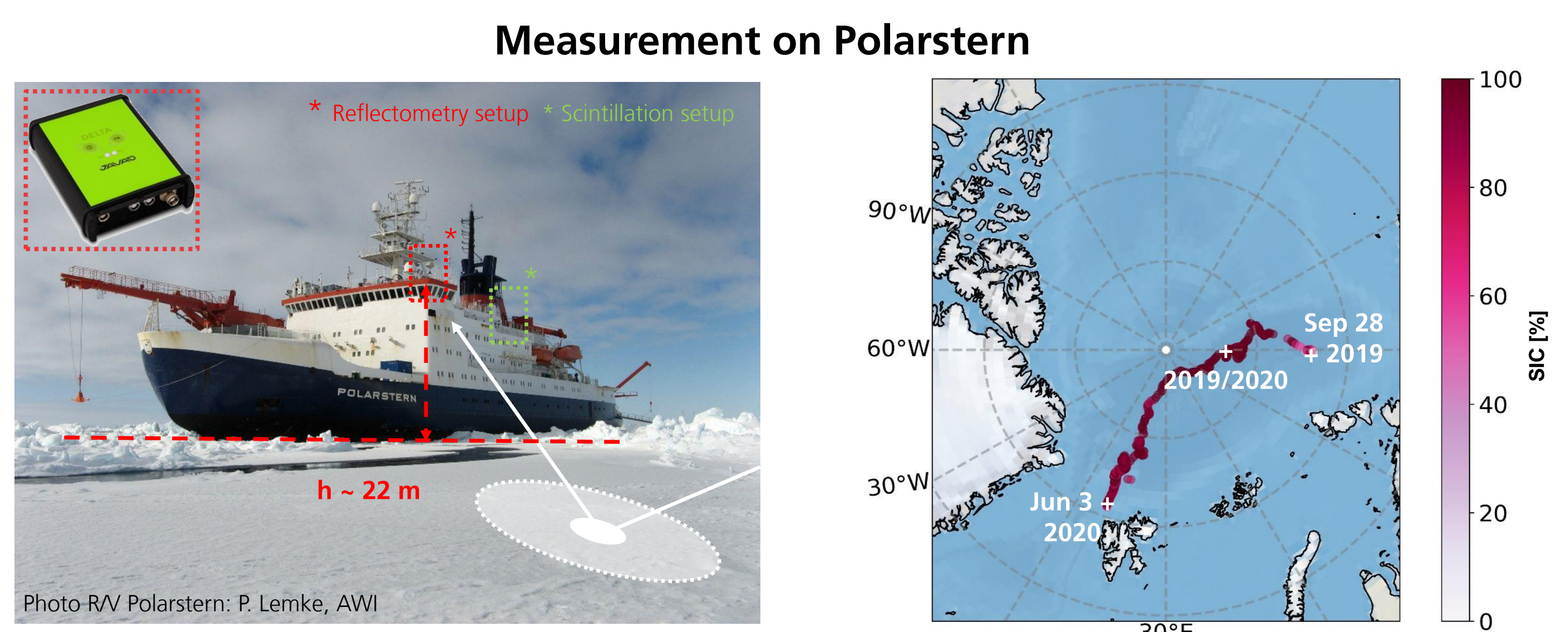


**Fig. 3, left panel:** Layout of measurements on *R/V Polarstern* for reflectometry and scintillation studies with portside view. Both setups run for one year during the MOSAiC expedition. **Right panel:** track of *Polarstern* between Sep 2019 and Jun 2020.

### Retrieval in Post-processing

The retrieval of relative permittivity estimates  $\epsilon$  comprises a hardware (on-board) processor and a software (post-) processor. The hardware processing involves antenna links with right- and left-handed polarization as well as the receiver that produces correlation amplitudes ( $i, q$ ) of the respective links. The software processing is based on the  $i, q$  amplitudes and separates direct and reflected signal power contributions in a first step. The reflection power (relative to the direct signal power) can be mapped over elevation angle and height, see examples from marginal ice zone (MIZ) and compact ice zone (CIZ) in **Fig. 3, left panel**. Sea surface reflection signatures appear in the given maps at the antenna height above reflector (here:  $\sim 22\text{m}$  above sea level). The reflection signatures typically cover elevations from the horizon ( $0^\circ$ ) to about  $30^\circ$  and depend on the different surface conditions (in MIZ and CIZ). Elevation profiles of reflectivity (reflected power relative to direct power) are derived (at the given height) as shown for MIZ (3 days) and CIZ (2 months) in **Fig. 3, right panel**. The applied processing concentrates on the  $10^\circ$ -to- $30^\circ$  elevation range for inverting the relative permittivity based on a linear fit of the profile. More details about the processing are found in Semmling et al. [2022].

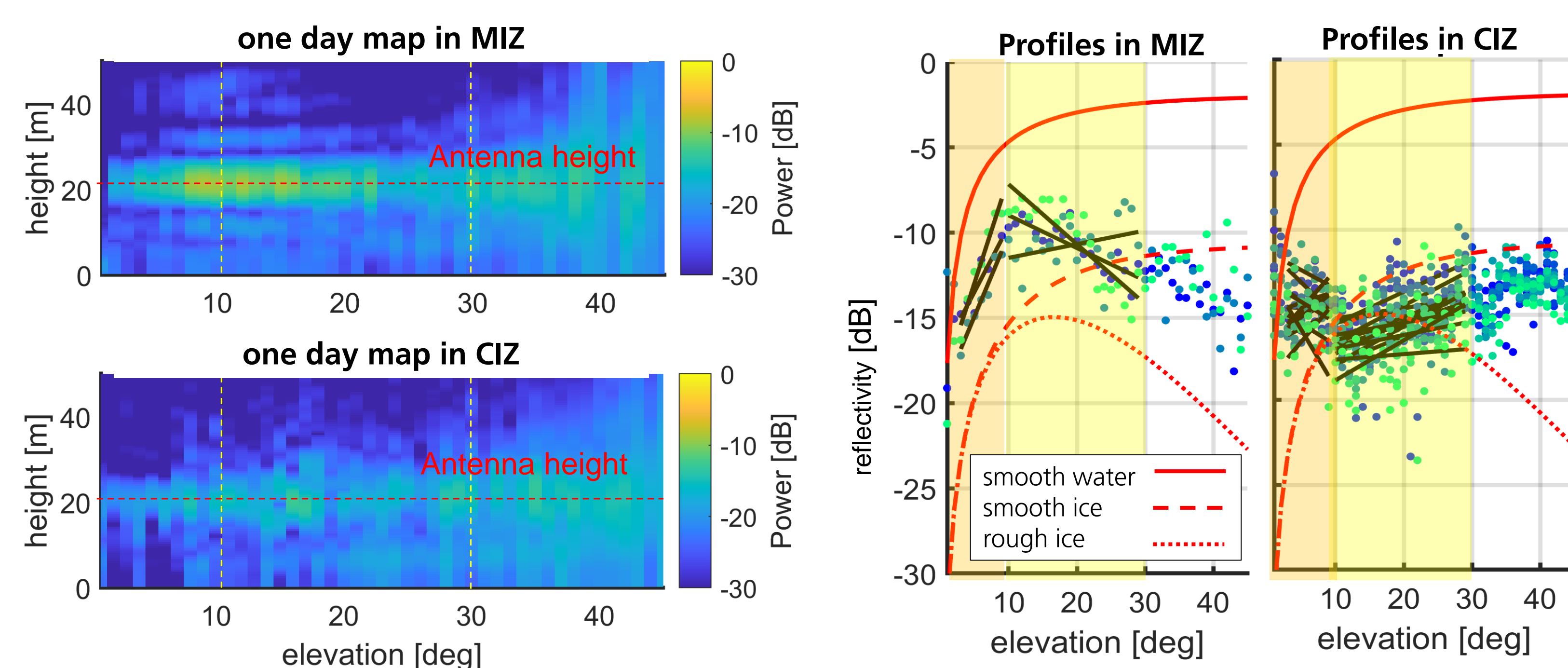


**Fig. 3, left panel:** reflection power map over reflector height and satellite elevation. Examples taken from marginal ice zone and compact ice zone. **Right panel:** reflectivity profiles derived for the respective zones, day of the profile is color-coded (blue – early to green – late), model predictions added (red curves).

## References

- Semmling et al. [2019]: "Sea Ice concentration derived from GNSS reflection measurements in Fram Strait". IEEE Trans. Geosci. Rem. Sens. 57.12, pp. 10350–10361. doi: 10.1109/TGRS.2019.2933911
- Munoz-Martin et al. [2020]: "Snow and Ice Thickness Retrievals Using GNSS-R: Preliminary Results of the MOSAiC Experiment". Remote Sensing 12, p. 4038. doi: 10.3390/rs12244038.
- Semmling et al. [2022]: "Sea-ice permittivity derived from GNSS reflection profiles: Results of the MOSAiC expedition". IEEE Trans. Geosci. Rem. Sens. 60, p. 4302416. doi: 10.1109/TGRS.2021.3121993.

## Scenarios for GNSS Reflectometry

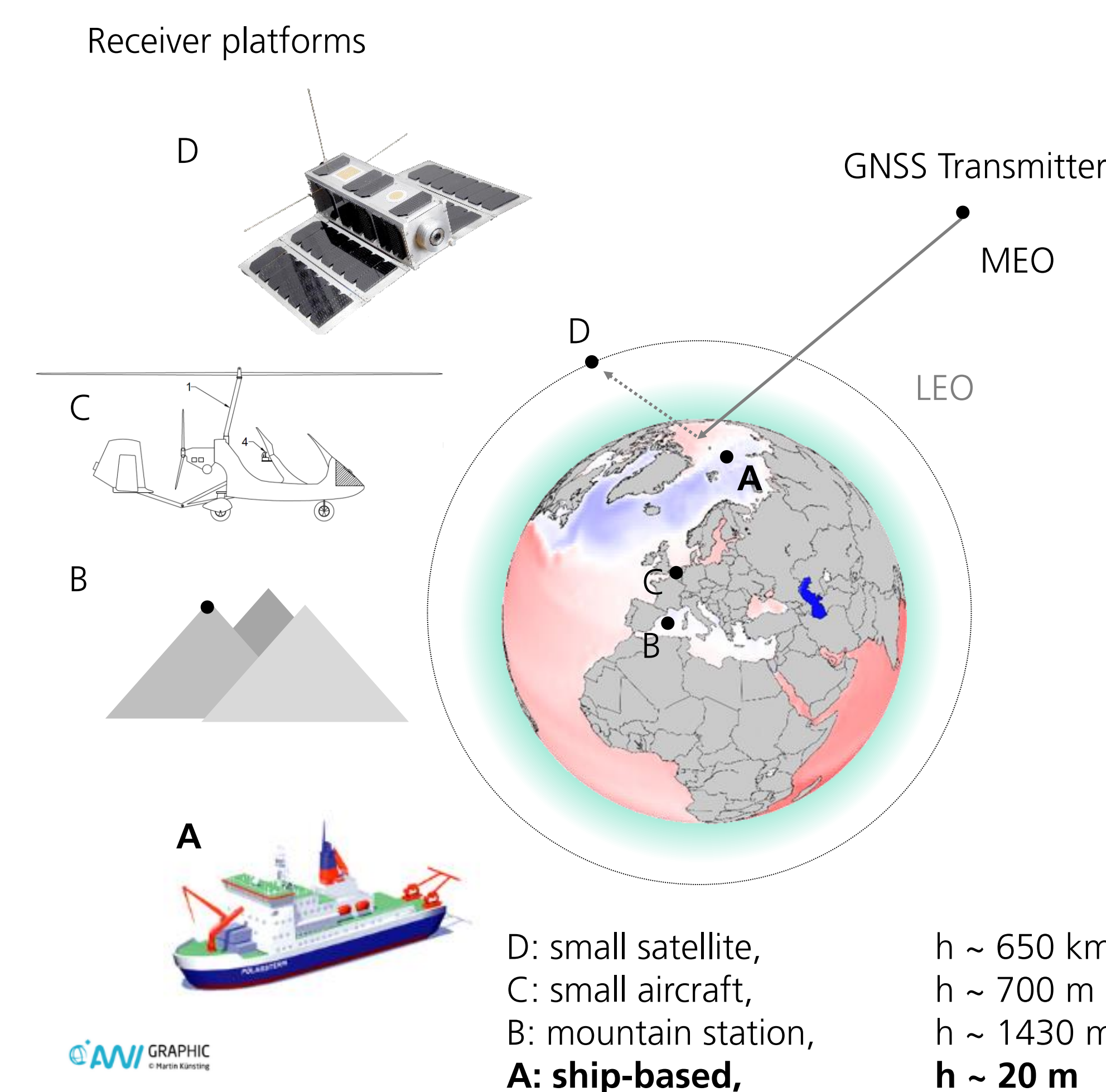


**Fig. 1:** Different receiver platforms for reflectometry scenarios that are currently investigated.

GNSS remote sensing techniques rely on the globally available L-band signals transmitted by Medium Earth Orbit (MEO) satellites. Most common techniques analyze the signal's propagation in the Earth's atmosphere (atmospheric sounding techniques) and the Earth-reflected signal (reflectometry techniques). Several scenarios for reflectometry are currently under research including receivers on ground/mountains, airborne, on satellite and also on ships. Examples are shown to the left in **Fig. 1**: based on ships in the Arctic (A), from a mountain station on Mallorca island (B), from a small aircraft at the French coast (C) and from a small satellite in the PRETTY mission for global observations (D). The over-arching goal of all these studies is a better understanding of the GNSS signal's interaction with the sea surface and atmosphere as well as a respective exploitation of GNSS observations for remote sensing.

The concept of sea-ice monitoring with ship-based observation is indicated in **Fig. 2** here to the lower left. Signals reach the ship-based receiver on the direct path (black ray) and on specular reflection paths (red rays). The power of the reflected signal depends (among other properties) on the permittivity of the reflecting surface. Water and sea ice are significantly different in their L-band relative permittivity and contrast in GNSS reflectivity estimates. Another important parameter of the reflection is the elevation angle  $\theta$ . Characteristics of reflectivity profiles over elevation have been investigated to estimate sea-ice properties: sea-ice concentration (SIC) [Semmling et al. 2019], sea-ice thickness [Munoz-Martin et al. 2020]. Here, we focus on the ice permittivity.

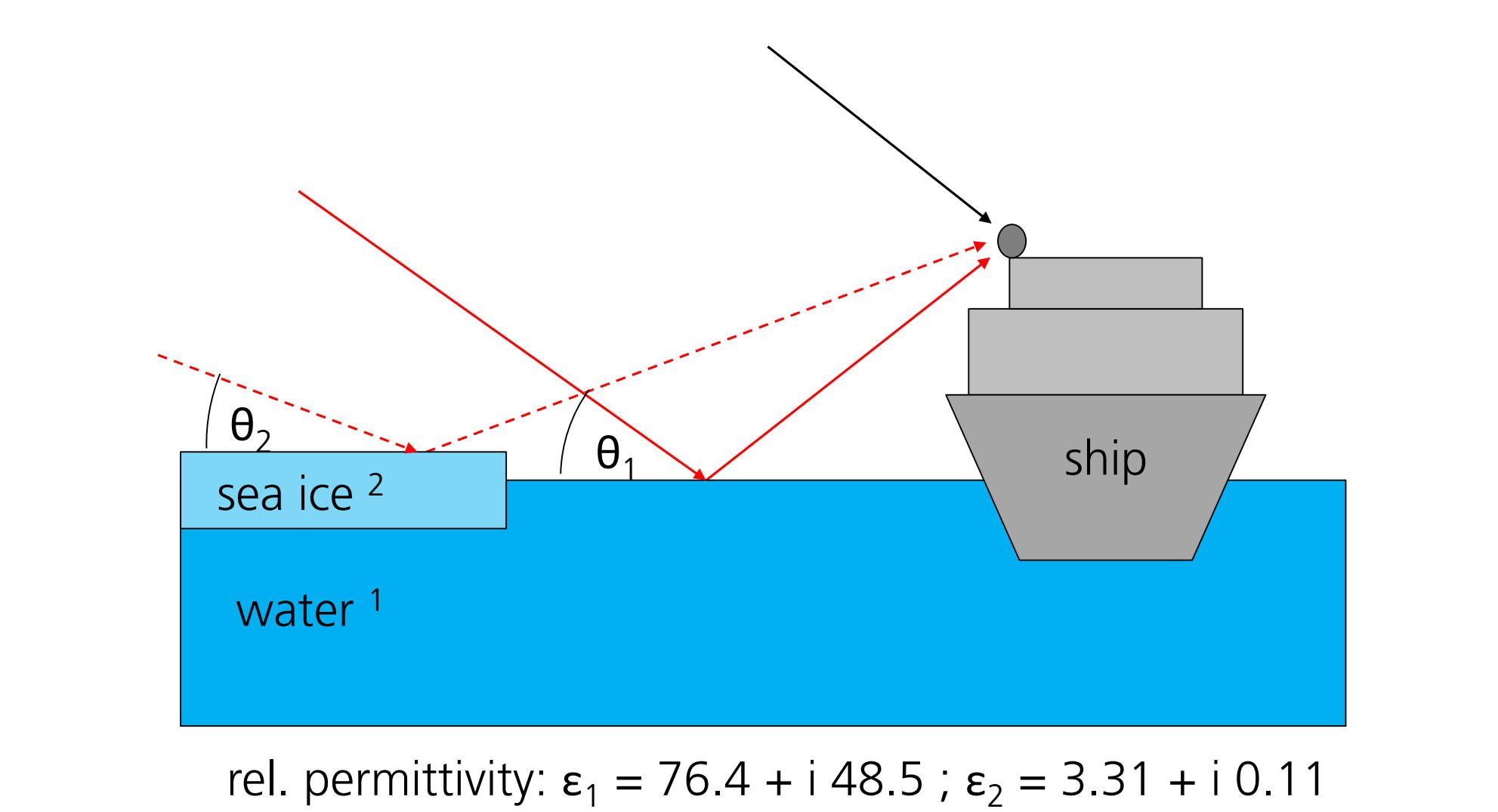


**Fig. 2:** Model of sea ice reflection for ship-based observation assuming bulk media without penetration.

## Results on Reflectivity and Relative Permittivity

The described processing was applied to the entire data set of the first drift period, cf. map in **Fig. 2**. The derived reflectivity profiles in **Fig. 3** (left panel) show typical features of bulk reflection (LH polarization) with moderate roughness effect in the MIZ: steep rise at lowest elevation (orange shaded) and slow fall at higher elevations (yellow shaded). Features of sea-ice penetration occur in the CIZ: anomaly of a constant to falling profile at lowest elevation (orange shaded). For more details see Semmling et al. [2022]. The linear fit in the mid-elevation range (yellow shaded) is most suitable for permittivity inversion. The anomaly at lower elevation and the roughness effect at higher elevations would, otherwise, require further corrections before inversion. **Fig. 4** presents results of  $\epsilon$  estimation (red markers) in the upper panel. The background color indicates the different periods of observation: gray in the CIZ (SIC = 100%), orange for lower SIC in the MIZ, during storm impact (SI) and in the transition zone (TZ) at the end of the first drift period. It is obvious that permittivity is increased ( $\epsilon > 5$ ) in MIZ and during SI when SIC < 100% (presence of water). However, low estimates ( $\epsilon < 3$ ) also occur in the TZ when SIC is decreasing. The reason for the TZ anomaly is not yet found. An increase of surface roughness or of sea-ice thickness could play a role.

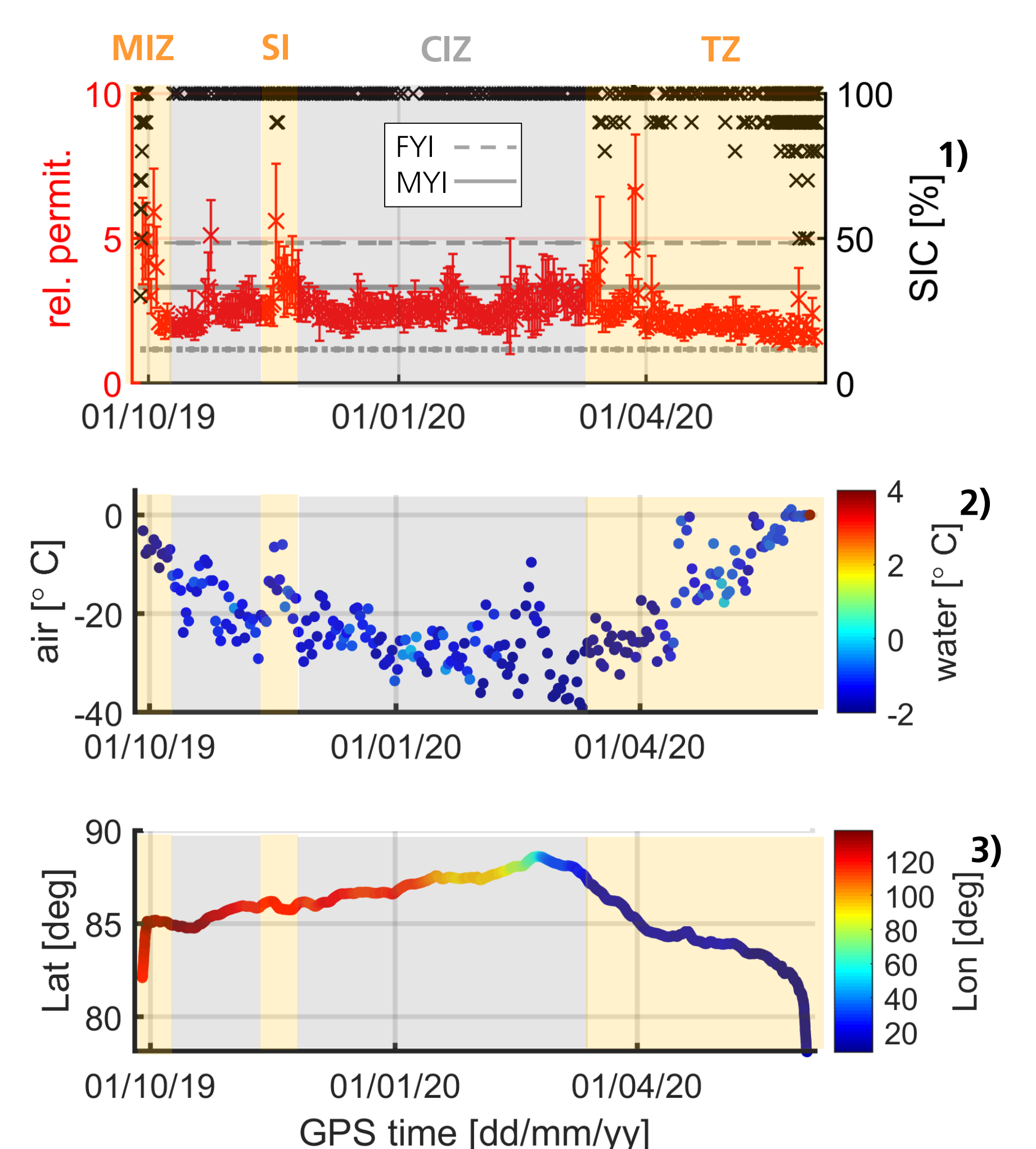


**Fig. 4, upper panel:** permittivity estimates (red), sea-ice concentration (black), **centre and lower panel:** temperatures (air, water) and location of ship (latitude, longitude), respectively. Sources: **1)** ASSIST protocol, in-situ data; **2)** DSHIP data base, AWI; **3)** GNSS based data, GFZ/DLR;

## Conclusion & Outlook

- Reflectivity profiles of the sea surface can be derived from a ship-based GNSS setup. The changing surface permittivity, when sea ice occurs, can be resolved from these (cross-polar, LH to RH) reflectivity results.
- A conclusion on sea-ice type only based on estimates  $\epsilon$  is not possible. Changes in SIC will impact estimation, cf. storm impact in Nov. 2019. SIC will significantly alter the results even if the ice type remains the same.
- A further study is on-going analyzing amplitude and phase fluctuations in the MOSAiC data set to study the impact of ionospheric irregularities. The use of GNSS observations in a ship-based scenario, in general, is more challenging (attitude changes, restricted visibility) than in more common ground-based scenarios. Additional processing can partly overcome these challenges to achieve valuable GNSS remote sensing observations from ships. Such data is relevant to improve sparse coverage over the oceans.

Acknowledgments: We grateful for the efforts of the *Polarstern* crew and AWI's technical and logistical efforts. IT and Werkstatt services at GFZ and DLR are kindly acknowledged that were essential to prepare the GNSS setups and to transfer the data. Thanks to Lars Kaleschke, Robert Ricker and Aikaterini Tavri for their on-site support.

Contact: M. Semmling  
DLR, Institute for Solar-Terrestrial Physics  
Kalkhorstweg 53, 17235 Neustrelitz, Germany  
Email: maximilian.semmling@dlr.de